Journal of Applied Polymer Science

Sunflower-Oil-Based Lecithin Organogels as Matrices for Controlled Drug Delivery

D. Satapathy, D. Biswas, B. Behera, S. S. Sagiri, K. Pal, K. Pramanik
Soft Materials and Medical Instrumentation Laboratory, Department of Biotechnology and Medical Engineering, National Institute of Technology, Rourkela, India
Correspondence to: K. Pal (E-mail: pal.kunal@yahoo.com)

ABSTRACT: In this study, we dealt with the development of lecithin-based organogels using sunflower oil as the apolar phase. Metronidazole (MZ) was used as a model drug. The organogels were characterized by microscopy (light and phase contrast), Fourier transform infrared spectroscopy, X-ray diffraction, differential scanning calorimetry, rheology, alternating-current impedance, hemocompatibility, antimicrobial analysis, and *in vitro* drug release. Microscopic analysis revealed the presence of spherical reverse micellar structures. There was an increase in the intermolecular hydrogen bonding among the gel components and crystallinity as MZ was incorporated into the organogels. The pH of the gel indicated that the gel may be nonirritant in nature and was hemocompatible. The release of MZ from the organogels followed Higuchi kinetics and was governed by anomalous or non-Fickian transport. The drug-loaded organogels showed antimicrobial activity against *Bacillus subtilis*, a Gram-positive bacteria. The preliminary results indicate that the developed organogel may be used as drug-delivery vehicle. © 2012 Wiley Periodicals, Inc. J. Appl. Polym. Sci. 000: 000–000, 2012

KEYWORDS: biocompatibility; biodegradable; biomaterials; drug delivery systems; micelles

Received 28 April 2012; accepted 21 August 2012; published online
DOI: 10.1002/app.38498

INTRODUCTION

The use of organogel-based formulations has been increasing for the past few years; this may be due to the easy method of preparation and inherent long-term stability of these products.[1,2] Organogels contain immobilized apolar liquids within a three-dimensional (3D) networked structure. The components that help in the gelation of the apolar liquids are known as *organogelators*. Commonly used organogelators include lecithin (LH), sterols, cholesterylanthraquinone derivatives, and fatty acid esters.[3] The 3D networked structure may either be a solid matrix or a fluid-filled matrix.[4] LH leads to the formation of fluid-filled reverse micellar structures, which, in turn, self-assemble to form 3D networked structures.[5–7] Depending on the nature of the apolar liquid, LH organogels may form either spherical micellar aggregates or wormlike tubular micellar aggregates.[8–12] The formation of the 3D networked structure is a spontaneous process attributed to the self-assembled supramolecular arrangement of surfactants.[13] The LH organogels are considered to be thermodynamically stable in nature; this, in turn, helps the gel maintain its structural integrity for a longer period of time. The chemistry of LH makes the organogels insensitive to moisture. The moisture-insensitive nature of the gels makes them resistant to microbial contamination.[14,15] LH, a zwitterionic phospholipid,[2] can be found abundantly in the biological system.[16] Because of the inherent biocompatibility, biodegradability, and nonimmunogenic nature of LH,[17] LH has been used extensively in the development of various food, pharmaceutical, and cosmetic products.[18] The use of LH organogels is very safe, even when they are applied for a long period of time; this may be due the previously mentioned properties.[19–22] LH organogels, because of their versatile structure, act as template vehicles by virtue of which they can accommodate a wide number of substances having diverse physicochemical natures.[15,23,24] Bioactive agents, whether with lipophilic, hydrophilic, or amphiphilic moieties, can be easily incorporated within LH organogels.[25] The permeation of the drug through the skin may be enhanced with various skin permeation enhancers (e.g., limonene and pluronic acid).[13,26,27] LH organogels, because of their unique architecture, help to hydrate the skin even in a lipid-enriched envioronment.[28,29] Sunflower oil (SO), a commonly used edible oil, is readily available in the market at much lower prices. Taking inspiration from this, we attempted to develop SO-based stable LH organogels for use as vehicles for various bioactive agents. Metronidazole (MZ) was used as a model drug to test the efficiency of the developed organogel.

EXPERIMENTAL

Materials

Soy lecithin (LH) and MZ were procured as a gift from VAV Life Sciences Pvt., Ltd. (Mumbai, India) and Aarti Drugs (Mumbai, India), respectively. SO was purchased from a local market. Dialysis tubing (molecular weight cutoff = 12–14 kDa) was purchased from Himedia (Mumbai, India). All of the experimental studies were carried out with double-distilled water.

Preparation of the Organogels

The optimization of the LH, SO, and water contents for the development of stable LH-based organogels was carried out by the alteration of the proportions of the components and the subsequent plotting of the ternary phase diagram. The samples were prepared by the dissolution of an accurately weighed amount of LH in a specified amount of SO; this mixture was stirred at 2000 rpm. Thereafter, water was added dropwise to the LH–SO mixture with continuous stirring until a specified amount of water was added (as calculated from the ternary phase diagram). Gelation was considered successful when the gels failed to flow under gravity on inversion of the vials.[30,31] On the basis of the preliminary studies, we found that the most stable organogel (LG) was formed when the LH/SO/water proportion was 22.5 : 35:42.5 wt %. The 1% w/w MZ (model drug)-loaded gel was prepared in the same manner, and this gel was named LGD. For microscopic studies, an LX organogel (with an LH/SO/water ratio of 22.5 : 35:30) was used. All of the samples were kept under refrigeration for further analysis.

Organoleptic Evaluation

Freshly prepared samples were observed for their color, odor, taste, appearance, and texture.

Microscopic Studies

A compound optical microscope (Leica DM 750 equipped with an ICC 50-HD camera, Wetzlar, Germany) and an inverted phase-contrast microscope (Olympus-INVI-TR attached to a Sony EPL-I digital camera, Philadelphia, USA) were used to analyze the microstructures of the samples. Attempts were made to understand the mechanism of formation of the LH organogels through the variation of the proportions of water in the LH organogels.

Size Distribution Analysis.

The size distribution of the reverse micellar particles were calculated with NI Vision 2010 software (National instruments, Austin, Texas, U.S). The background noise of the images was removed by the background subtraction method and was subsequently thresholded to obtain binary images. The conjoining particles, if any, were separated with an erosion algorithm. This was followed by the implementation of a convex hull algorithm, which helped not only to remove the holes within the particles but also to enclose any improperly closed particles. Thereafter, the small particles, often associated with the noise incorporated by thresholding, were removed. The border objects were also removed to prevent the incorporation of erroneous results. A separate object algorithm was then applied to separate particles that might have joined after the convex hull algorithm was applied. Circular particles having a Heywood circularity factor in the range of 0.8–1.2 were then selected for the determination of the diameter of the particles.

Figure 1. LG organogel. [Color figure can be viewed in the online issue, which is available at wileyonlinelibrary.com.]

Fourier transform infrared (FTIR) Analysis

Infrared spectroscopy of the samples was performed with an attenuated total reflectance–FTIR instrument (Alpha-E, Bruker, Karlsruhe, Germany). The raw materials and representative organogels were scanned in the range 4000–500 cm^{-1} to understand the interactions among the components of the organogel.

X-Ray Diffraction (XRD) Analysis

XRD analyses of the samples were carried out with a Philips XRD-PW 1700 (Rockville, MD). Cu Kα radiation was used as the source, and the instrument was operated at 35 kV and 30 mA. Samples were scanned in the 2θ range 10–50° at a rate of 2°/min.

Thermal Analysis

The organogels were subjected to differential scanning calorimetry (DSC) to analyze thermal analysis of LG and LGD with a DSC-200-F3 MAIA instrument (Netzsch, Wittelsbacherstrasse, Germany) over a temperature range of 25–90°C at a heating rate of 1°C/min. An accurately weighed sample (10–15 mg) was used for the analysis. The samples were placed in aluminum (Al) crucibles and hermetically sealed with a pierced Al lid.

Rheological Studies

A controlled stress cone–plate viscometer (Bohlin Visco 88, Malvern, United Kingdom) was used to determine the rheological properties of the LG and LGD organogels. All measurements were done with freshly prepared samples. A cone with an angle of 5.4° and having a diameter of 30 mm was used. The gap between the cone and plate was set at 0.15 mm. The whole procedure was carried out at room temperature.

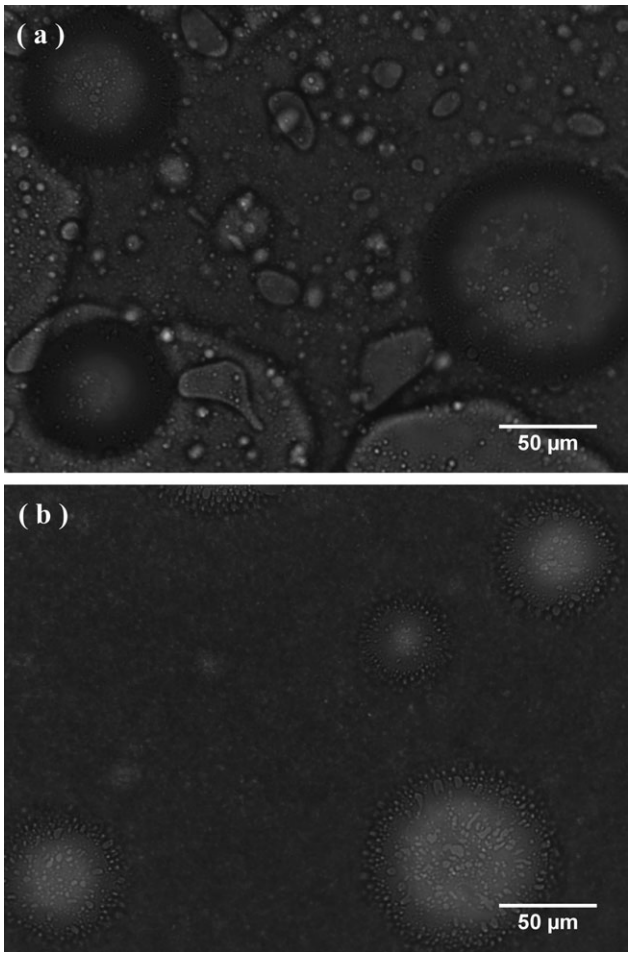

Figure 2. Light micrographs of the LG organogels with various water concentrations: (a) 30 and (b) 42.5% w/w.

Spreadability Studies

The spreadability values of the LG, LGD, and marketed formulation Metrogyl (MZ1) gels were determined as per a reported method.[32] Predetermined amounts of the samples (0.5 g) were placed between two glass plates of equal weight and area. The initial diameter (D_1) was noted. Thereafter, various weights (10, 20, 50, and 100 g) were placed over the upper slide. The final diameter (D_2) was noted over a period of 60 s. The spreadability of the formulations was reported as the percentage spreadability as per eq. (1):

$$\text{Spreadability} = \frac{D_2 - D_1}{D_1} \times 100 \qquad (1)$$

Disintegration Studies

The disintegration of the LG and LGD encapsulated gelatin capsules was carried out with a tablet disintegration test apparatus (model 901, Electronics India, Mumbai, India). For this study, 0.4 g of each of LG and LGD gels was poured into the hard gelatin capsules. The capsules containing gels were placed in the disintegration test apparatus. Double-distilled water maintained at 37°C was used as the disintegrating media. The time taken for the complete disintegration of the capsules and its contents, as indicated by the absence of any component (capsule or gel) of the formulation in the disintegration basket, was noted as the disintegration time.

Alternating-Current (ac) Impedance Analysis

The ac impedance of the LG and LGD organogels was measured in the frequency range of 100 Hz to 5 KHz with an impedance analyzer built in-house. In this study, a low-amplitude current of various frequencies was passed through the samples with stainless steel electrodes. The corresponding changes in voltage were recorded with LABVIEW-2010 software (National Instruments, Austin, Texas, U.S.A.).

In Vitro Drug-Release Studies

A vertical diffusion cell arrangement was used for the drug-release study. An accurately weighed 1 g of LGD was placed in the donor compartment, which was separated from the receptor compartment by a dialysis membrane (molecular weight cutoff = 60 KDa, Himedia), and the receptor fluid, which was maintained at 37 ± 0.5°C, was stirred at 100 rpm on a magnetic stirrer (Remi India, Ltd., Mumbai, India). Double-distilled water was used as the dissolution media. To ensure sink conditions, the volume of the receptor compartment was completely replaced with the fresh dissolution media at a predetermined

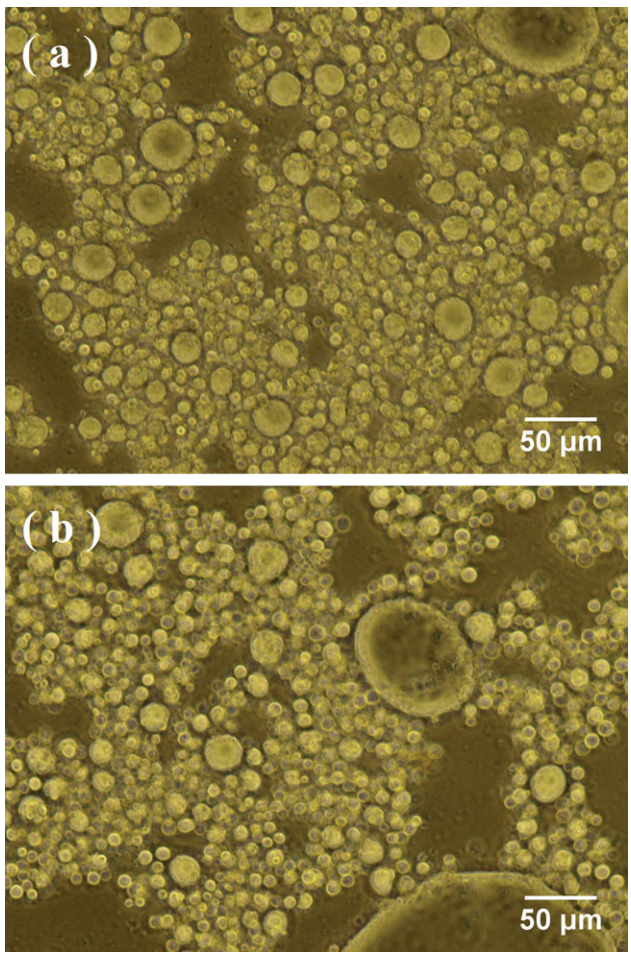

Figure 3. Phase-contrast micrographs of LH organogels having water concentrations of (a) 30% w/w (LX gel) and (b) 42.5% w/w (LG gel). [Color figure can be viewed in the online issue, which is available at wileyonlinelibrary.com.]

Applied Polymer SCIENCE

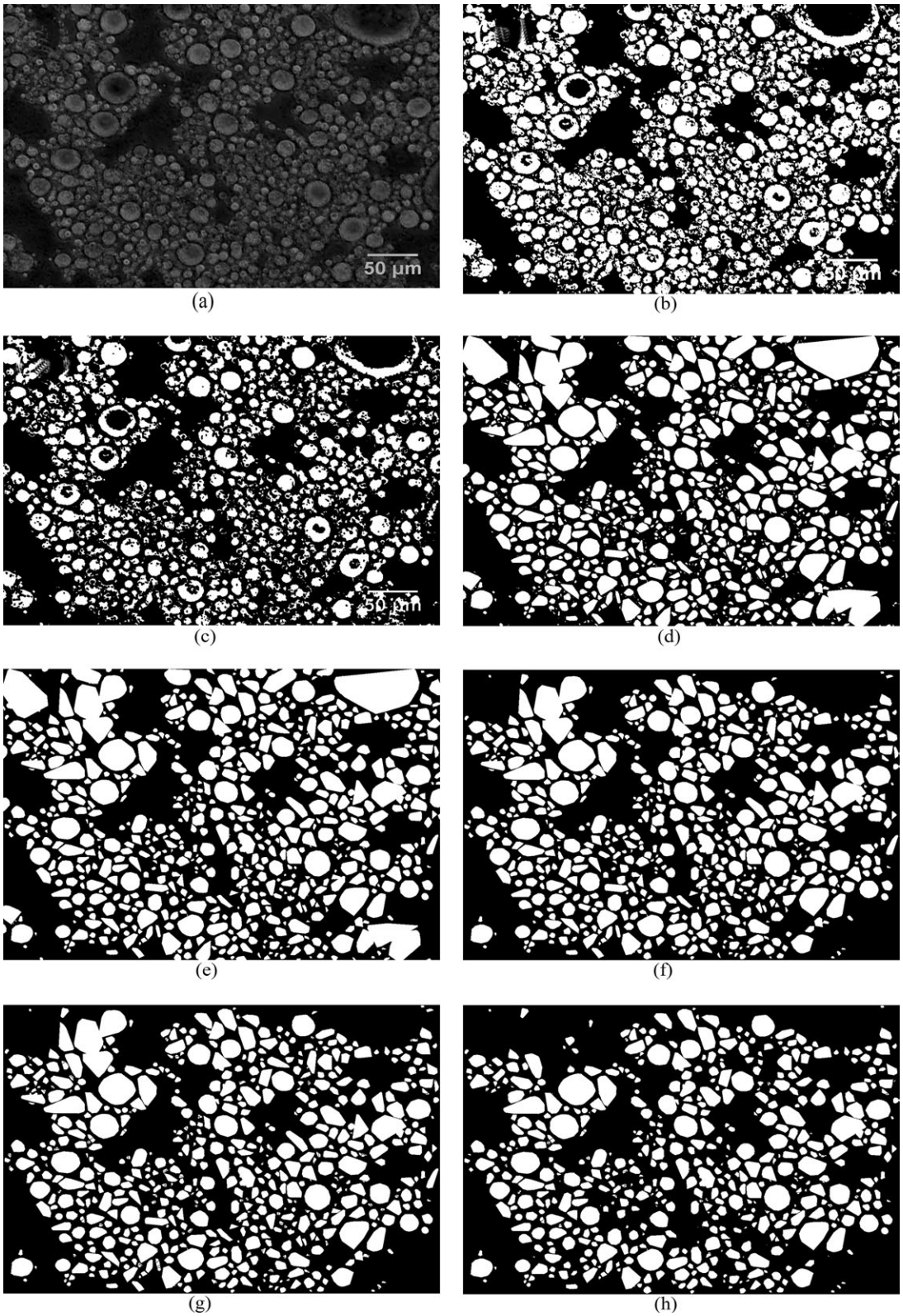

Figure 4. Sequentially processed microscopic images of the LX gel: (a) color plane extraction, (b) threshold, (c) erosion, (d) convex hull, (e) removal of small particles, (f) removal of border objects, (g) separation of objects, and (h) Heywood circularity factor.

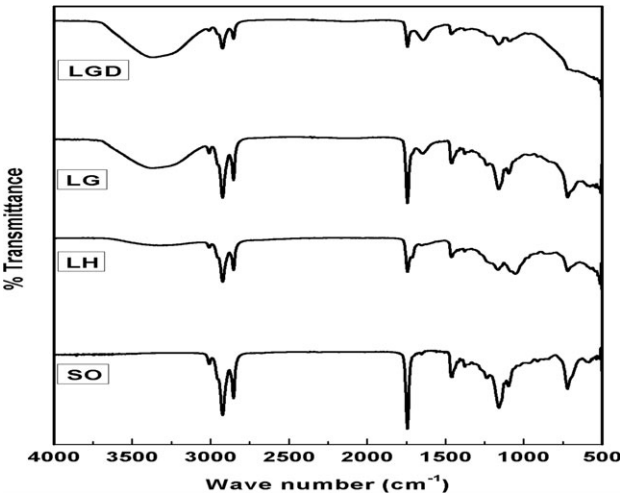

Figure 5. FTIR spectra of the LH organogels.

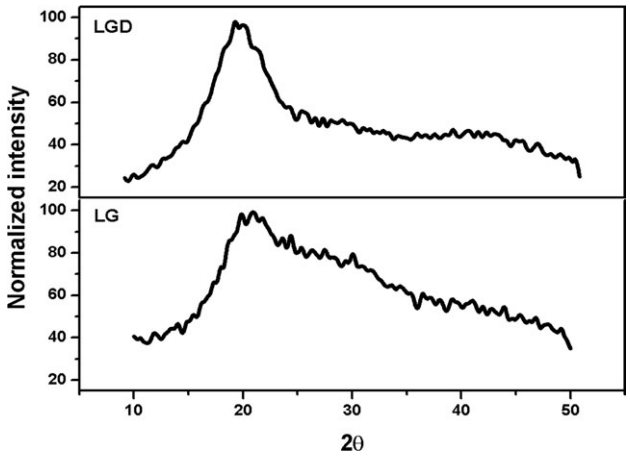

Figure 6. XRD analysis of the LG and LGD organogel samples.

interval of 30 min. The study was conducted for 9 h. The dissolution media was spectrophotometrically analyzed at a maximum wavelength of 321 nm. The experiments were carried out in duplicate.

pH Measurement

The pH of the samples were detected with a digital ATC pH meter (model 132E, EI Instruments, Mumbai, India) at room temperature. We measured the pH of the organogels by bringing the probe of the pH meter in contact with the samples. The pH of topical drug-delivery preparations should lie in the range 4.5–6 (skin pH) to prevent irritation to the skin.[33]

Hemocompatibility Test

A hemocompatibility test was carried out to determine the extent of hemolysis in the presence of the organogel samples. The test was done as per a method described elsewhere.[34–42]

Antimicrobial Studies

The antimicrobial efficacy of the LGD organogel was analyzed against *Bacillus subtilis* by the bore-well method. The microbial culture plates were incubated at 37°C for 24 h, and the resulting zone of inhibition was measured.[42,43]

RESULTS AND DISCUSSION

Preparation of the Organogels

LH was dissolved in SO with stirring at 2000 rpm to obtain a homogeneous solution. Gel formation was confirmed by the inverted tube method (Figure 1).[30] The samples were regarded as organogels if they did not flow.[44] LH organogels started forming when the water concentration reached 30% w/w at the critical gelator concentration of LH (22.5% w/w), and the gels were regarded as LX organogels. However, the LX gels were found to destabilize 1 week after preparation. The preliminary results indicate that the LG organogel was the most stable gel, and hence, it was used for further studies.

Table I. AUC of the —OH Peaks of the FTIR Spectra of the Samples

Sample	AUC of the —OH stretching peak
LH	39.46
LG	89.61
LGD	165.87

Organoleptic Evaluation

The LG organogel was light brown in color. The gel was oily to touch and smooth in texture and had a bland taste.

Microscopic Studies

The micrographs of the organogel showed the presence of spherical reverse micellar structures having sizes in the range 30–80 μm. With increasing proportion of water, there was a subsequent increase in the micellar structures with improved organization (Figure 2). Phase-contrast micrographs showed that in addition to larger reverse micellar structures (as seen under a light microscope), there were numerous small reverse micellar structures, which were in the range 5–30 μm (Figure 3). The spherical reverse micellar structures reorganized themselves to form a 3D network. The formation of a well-organized 3D network structure as the proportion of water was increased may explain the stable nature of the LG gel.

The processed images for the size distribution analysis of the LX gel after each step in the NI Vision software are shown in Figure 4. The results of the particle size measurements were exported to an Microsoft Excel file. The results were used to figure out the particle size distribution in the gels (Figure 3). The results show that the maximum number of particles for LX and LG had sizes of 2.75 and 2.28 μm, respectively. Also, the cumulative size distribution of the particles indicated that 50% of the particles of LX and LG were 2.4 and 2.04 μm, respectively. The smaller sizes of the particles of the LG gel may have been due to the formation of a more ordered and compact networked structure, which in turn, improved the stability of the LG gel.

Table II. XRD Analysis of the LG and LGD Organogels

Sample	AUC	fwhm
LG	3057.29	28.94
LGD	1203.72	11.54

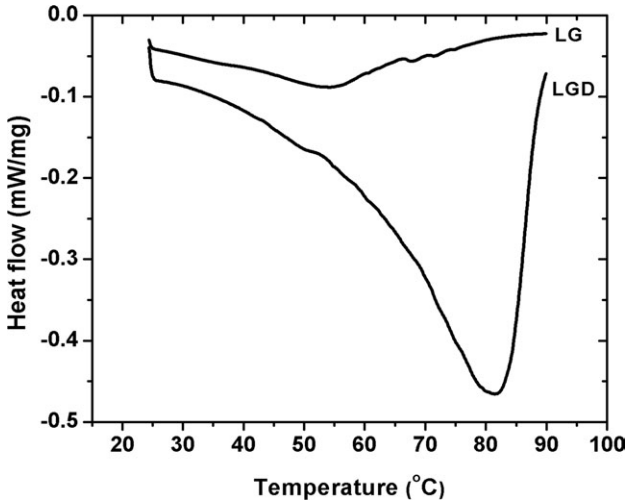

Figure 7. DSC thermogram of the LG and LGD organogel samples.

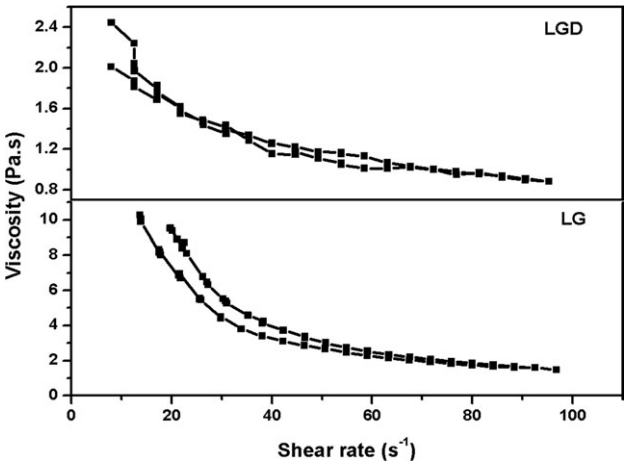

Figure 8. Plot of the viscosity versus shear rate of the LG and LGD organogels showing shear-thinning behavior.

FTIR Analysis

The IR spectra of the SO, LH, LG, and LGD are shown in Figure 5. LH, LG, and LGD exhibited an absorption band corresponding to O—H stretching at 3500 cm^{-1}. The intensity of the peak corresponding to the O—H stretching vibration in LG increased with the addition of the drug MZ. This may have been due to the chemical ordering of LGD due to the dominance of intermolecular hydrogen bonding.[45] There was no significant difference in the spectral pattern of the SO, LH, LG, and LGD in the rest of their spectra; this indicated that the chemical functionality of the gel components was conserved. The comparative increase in the intermolecular hydrogen bonding among the gel components was studied by the calculation of the area under the curve (AUC) obtained with the stretching of the O—H bond (Table I).[46,47] The increase in the AUC of the O—H stretching vibration was in the order LH < LG < LGD; this indicated that intermolecular hydrogen bonding was highest in the LGD and was followed by LG and LH, respectively.

XRD Analysis

The XRD patterns of the LG and LGD gels are shown in Figure 6. The XRD pattern indicated that there was an increase in the crystallinity of the LG gel with the incorporation of MZ into the LG gel. The increase in the crystallinity was confirmed by a decrease in the AUC and the full width at half-maximum (fwhm) of the LGD gel as compared to the LG gel (Table II). This increase in the crystallinity may have been due to the increase in the intermolecular hydrogen bonding in the LGD gel, as was evident from the FTIR studies.[48]

Table III. T_m, Enthalpy, and Entropy Data Obtained from the DSC Curves of the Organogels

Sample	T_m (°C)	ΔH^a (J/g)	ΔS (mJ g^{-1} K^{-1})
LG	52.6	−29.77	638.8
LGD	81.5	−266.3	−326.7

T_m, melting temperature.
[a]The negative sign of the ΔH values is due to endothermic convention.

Thermal Analysis

The thermal properties of the LG and LGD gels were studied with a differential scanning calorimeter in the temperature range 25–90°C. The results of thermal scanning are shown in Figure 7 and Table III. The LG gel showed an endothermic peak at 52.6°C, which may have been due to the gel-to-sol transition of the gel. The gel-to-sol transition of the LGD gel was found at a much higher temperature (81.5°C). The area under an endothermic peak is often associated with a change in enthalpy (ΔH).[49,50] The thermograms of LG and LGD showed that the AUCs of the glass-transition temperatures of the LGD gels were higher than those of the LG gels.[51] This suggested that there was an increase in the stability of the LG gels as MZ was incorporated within its structure. The increase in the ΔH values were associated with the subsequent decrease in the ΔS (change in entropy) values (associated with the degree of disorderliness).[52–54] This suggested that the LGD gel had a more ordered structure than the LG gels; this was also evident from the XRD studies.[55]

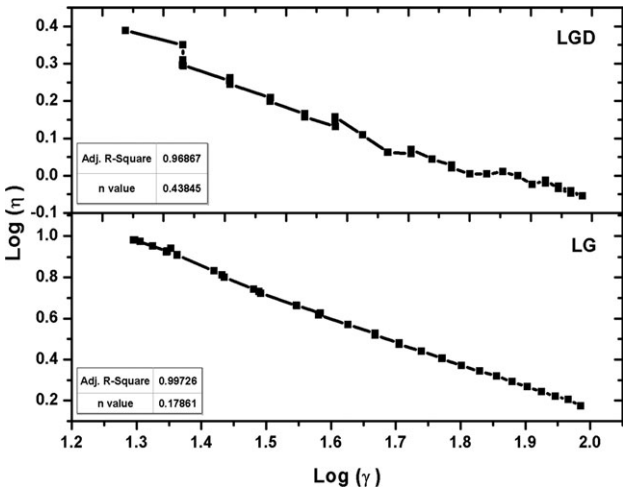

Figure 9. Plot of the viscosity versus shear rate (log–log scale) of the LG and LGD organogels.

Table IV. Power Law Parameters

Sample	n	r^2	Flow type
LG	0.17	0.99	Pseudoplastic
LGD	0.44	0.96	Pseudoplastic

Rheological Studies

The Ostwald–de Wale power law mathematical model (eq. 2) is an important tool for the rheological analysis of gel-based systems.[56]

$$\eta = K\gamma^{n-1} \quad (2)$$

where η is the shear viscosity, K is the consistency index, n is the power law index, and γ is the shear rate.

The viscosity profiles of the LG and LGD gels are shown in Figures 8 and 9. The shear-thinning behavior, a decrease in the viscosity with increasing shear rate, of the gels was quite evident from the viscosity profiles; this suggested non-Newtonian flow characteristics of the gels. The shear-thinning phenomenon is considered an essential parameter for topical application of the formulation.[23] This ensures the formation of a thin layer of the gel when it is applied over the skin surface, which in turn, results in the efficient delivery of bioactive agents at the site of application.[57] Also, the semisolid consistency of the formulation at low shear rates ensures long-term stability of the formulation during storage.[58] The n values calculated from the viscosity profiles of LG and LGD were found to be 0.17 and 0.44, respectively (Table IV). The value of $n < 1$ suggested that the gels followed a pseudoplastic rheological behavior.[59]

Spreadability Studies

The percentage spreadability with respect to various weights is shown in Figure 10. The percentage spreadability of the LG, LGD, and MZ1 varied in the ranges 15–25, 25–50, 55–86, and 75–95% when 10g, 20g, 50g and 100g were applied, respectively. There was an increase in the spreadability indices as the applied load was increased (Table V). The gels were found to be evenly spread without any phase separation. This indicated that the gels had good structural integrity and may be used as vehicles for topical and transdermal drug delivery.[60,61] The results suggested that the LG and LGD gels were more spreadable than MZ1, the marketed formulation.

Disintegration Studies

The disintegration of the capsules containing the LG and LGD gels was completed in a span of 5 min. The presence of MZ in the gels did not affect the disintegration of the gels. The study indicated that the encapsulated LG and LGD gels may be used for the oral delivery of bioactive agents.

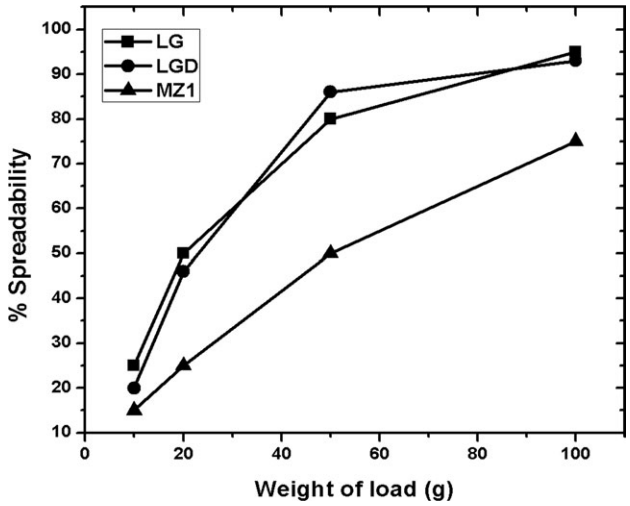

Figure 10. Plot showing the spreadability of the LG, LGD, and MZ1 organogels.

ac Impedance Analysis

The gels were found to be electrically conductive and dependent on the frequency of the injected current. The bulk resistance of the gels was measured to determine the conductance of the gels. There was a decrease in the impedance of the gels as the frequency of the injected current was increased (Figure 11). This suggested that the capacitive component was dominant in the gels compared to the inductive component.[62] LGD had a higher impedance than LG. This was quite understandable and may have been due to the highly ordered crystalline structure of LGD compared to that of LG.[63]

In Vitro Drug-Release Studies

The drug-release profile of LGD is shown in Figure 12. The amounts of MZ released from LGD and MZ1 were 89.12 and 89.37%, respectively, at the end of 9 h. This suggested that the drug-release profile of LGD was comparable to that of the marketed formulation. The correlation coefficient (r^2) was used to determine the best fit model (Table VI). The release kinetic studies indicated that the release pattern of the drug followed Higuchian kinetics; this suggested that the diffusion of MZ from the gel matrix was the rate-controlling parameter in the drug release. However, the Korsmeyer–Peppas model indicated that the release exponent n was 0.6; this suggested an anomalous or non-Fickian diffusion. We assumed from the results that the release of MZ from the gels was governed by more than one

Table V. Spreadability Data of the Samples

	Spreadability ($cm^2/g^{1/2}.s$)			
Sample	10 g	20 g	50 g	100 g
LG	0.018617	0.029255	0.033156	0.05495
LGD	0.012557	0.013164	0.0185026	0.0215875
MZ1	0.0081918	0.01515421	0.02068594	0.0243611

Applied Polymer SCIENCE

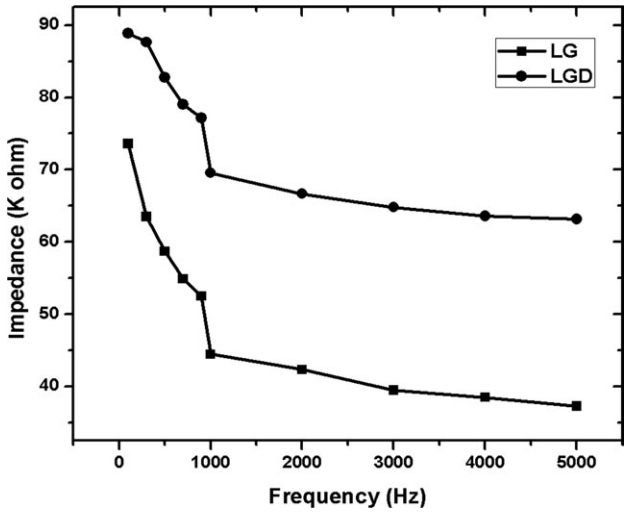

Figure 11. Impedance analysis of the LG and LGD organogel samples.

process.[64] In contrast to LGD, the drug release from MZ1 indicated that the release pattern was Higuchian kinetics with Fickian diffusion.

pH Measurement

The pH of the organogel was found to be 6.3 ± 0.30. This indicated that the gel may be nonirritating in nature.[42,65–68]

Hemocompatibility Test

The hemocompatibility test was done to study the disruption of red blood cells in the presence of the gel leachate. The presence of noncompatible leachant into a leachate resulted in the disruption of the red blood cells and stimulated the release of hemoglobin pigment into the solution.[69] The amount of hemoglobin released was then measured spectrophotometrically. The percentage hemolysis of both of the gels was found to be less than 5% (LG: 0.973 ± 1.2, LGD: 1.892 ± 1.2); this indicated that the gels were highly hemocompatible as per the literature.[42]

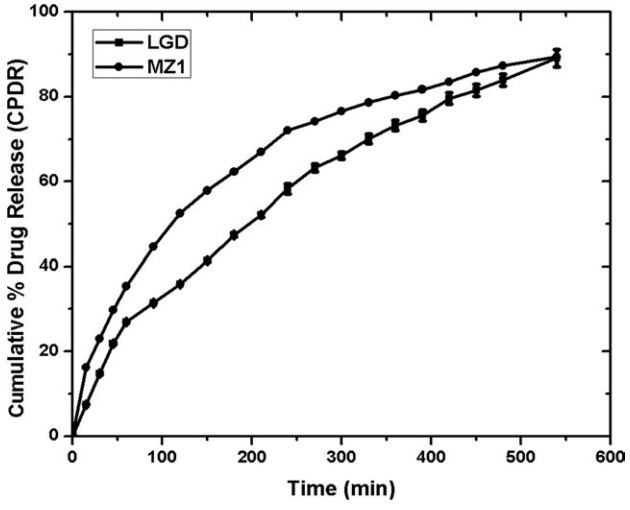

Figure 12. Cumulative percentage drug release values for the LGD and marketed gels as a function of time.

Table VI. Kinetics of *In Vitro* Drug Release

	Zero-order		Higuchi model		Korsmeyer–Peppas model	
Sample	r^2	k_0	r^2	k_H	r^2	n
LGD	0.8580	0.1977	0.9852	0.0375	0.9864	0.60
MZ1	0.5247	0.2192	0.9718	0.0426	0.9843	0.48

k_0, zero order rate constant; k_H, Higuchian constant.

Table VII. Zone of Inhibition Obtained in *B. subtilis*

Sample	Zone of inhibition (cm)
LG	Nil
LGD	2.00 ± 0.54
MZ	3.00 ± 0.45
MZ1	2.50 ± 0.21

Antimicrobial Studies

The antimicrobial efficiency results of the developed and marketed formulations are tabulated in Table VII. LG and MZ were used as negative and positive controls, respectively. The antimicrobial activities of LGD and MZ1 against *B. subtilis* were found to be statistically insignificant ($p < 0.05$). The blank gel did not show any antimicrobial activity; this suggested that the zone of inhibition was due to the incorporated drug only.

CONCLUSIONS

In this article, we have reported the successful development of LH- and SO-based organogels. The preliminary study suggested that the developed formulation has a great potential for use as a carrier for bioactive agents. The organogels were easy to prepare and had good physicochemical properties. The shear-thinning behavior of these gels indicated that the gels may be easily spreadable and hence may be used for topical application. The increase in the thermal stability of the drug-incorporated organogels (LGD) allowed them to retain their physicochemical and structural properties upon long-term storage and transport. The developed organogels did not elicit any adverse reactions against red blood cells (RBC) membranes; this indicated probable biocompatibility. The encapsulation of the LG and LGD gels within the gelatin capsules may help to mask the taste of the drugs dispersed within the gels and hence may be used as a formulation for the oral delivery of bioactive agents. The use of edible oil for formulating LH-based organogels may open up a new area for the oral delivery of pharmaceutical and nutraceutical agents. In the this article, we have reported the development of an LH organogel formulation consisting of only 22.5% LH. This is much lower than the previously reported LH concentrations (60%) used for the development of LH organogels.[70]

ACKNOWLEDGMENTS

The authors acknowledge logistical support from the National Institute of Technology, Rourkela, India. They also acknowledge funds leveraged from a project sanctioned by the Department of Biotechnology, Government of India (contract grant number BT/PR14282/PID/06/598/2010).

REFERENCES

1. Murdan, S.; Gregoriadis, G.; Florence, A. T. *Eur. J. Pharm. Sci.* **1999**, *8*, 177.
2. Vintiloiu, A.; Leroux, J. C. *J. Controlled Release* **2008**, *125*, 179.
3. Toro-Vazquez, J.; Morales-Rueda, J.; Dibildox-Alvarado, E.; Charo-Alonso, M.; Alonzo-Macias, M.; González-Chávez, M. *J. Am. Oil Chem. Soc.* **2007**, *84*, 989.
4. Terech, P.; Weiss, R. G. *Chem. Rev.* **1997**, *97*, 3133.
5. Scartazzini, R.; Luisi, P. L. *J. Phys. Chem.* **1988**, *92*, 829.
6. Schurtenberger, P.; Scartazzini, R.; Magid, L. J.; Leser, M. E.; Luisi, P. L. *J. Phys. Chem.* **1990**, *94*, 3695.
7. Luisi, P.; Scartazzini, R.; Haering, G.; Schurtenberger, P. *Colloid Polym. Sci.* **1990**, *268*, 356.
8. Capitani, D.; Segre, A. L.; Dreher, F.; Walde, P.; Luisi, P. L. *J. Phys. Chem.* **1996**, *100*, 15211.
9. Shchipunov, Y. A.; Schmiedel, P. *Langmuir* **1996**, *12*, 6443.
10. Aliotta, F.; Vasi, C.; Lechner, R.; Ruffle, B. *Phys. B: Condens. Matter* **2000**, *276*, 347.
11. Angelico, R.; Ceglie, A.; Colafemmina, G.; Lopez, F.; Murgia, S.; Olsson, U.; Palazzo, G. *Langmuir* **2005**, *21*, 140.
12. Schurtenberger, P.; Peng, Q.; Leser, M.; Luisi, P. L. *J. Colloid Interface Sci.* **1993**, *156*, 43.
13. Shchipunov, Y. A. *Colloids Surf. A* **2001**, *183*, 541.
14. Shumilina, E.; Khromova, Y. L.; Shchipunov, Y. A. *Russ. J. Phys. Chem.* **2000**, *74*, 1083.
15. Kumar, R.; Katare, O. P. *AAPS Pharmscitech* **2005**, *6*, 298.
16. Shchipunov, Y.; Krekoten, A. *Colloids Surf. B* **2011**, *87*, 203.
17. Dreher, F.; Walde, P.; Walther, P.; Wehrli, E. *J. Controlled Release* **1997**, *45*, 131.
18. Ofsthun, N. J. Kirk–Othmer Encyclopedia of Chemical Technology; John Wiley & Sons, Inc.: New york, USA, **2000.**
19. Dreher, F.; Walde, P.; Walther, P.; Wehrli, E. *J. Controlled Release* **1997**, *45*, 131.
20. Dreher, F.; Walde, P.; Luisi, P.; Elsner, P. Skin Pharmacology and Physiology; Karger Publishers: Basel, Switzerland, **1995**; p 640.
21. Cevc, G.; Blume, G.; Schätzlein, A.; Gebauer, D.; Paul, A. *Adv. Drug Delivery Rev.* **1996**, *18*, 349.
22. Dreher, F.; Walde, P.; Luisi, P.; Elsner, P. *Skin Pharmacol. Physiol.* **1996**, *9*, 124.
23. Shchipunov, Y. A.; Hoffmann, H. *Rheol. Acta* **2000**, *39*, 542.
24. Jerke, G.; Pedersen, J. S.; Egelhaaf, S. U.; Schurtenberger, P. *Langmuir* **1998**, *14*, 6013.
25. Hadgraft, J. *Int. J. Pharm.* **1999**, *184*, 1.
26. Willis-Goulet, H. S.; Schmidt, B. A.; Nicklin, C. F.; Marsella, R.; Kunkle, G. A. *Vet. Dermatol.* **2003**, *14*, 83.
27. Papadimitriou, V.; Pispas, S.; Syriou, S.; Pournara, A.; Zoumpanioti, M.; Sotiroudis, T. G.; Xenakis, A. *Langmuir* **2008**, *24*, 3380.
28. Willimann, H.; Walde, P.; Luisi, P.; Gazzaniga, A.; Stroppolo, F. *J. Pharm. Sci.* **1992**, *81*, 871.
29. Bhatnagar, S.; Vyas, S. *J. Microencapsulation* **1994**, *11*, 431.
30. Maity, G. C. *J. Phys. Sci.* **2007**, *11*, 156.
31. Shaikh, I. M.; Jadhav, S.; Jadhav, K.; Kadam, V.; Pisal, S. *Current Drug Delivery* **2009**, *6*, 1.
32. Barakat, N. *Asian J. Pharm.* **2010**, *4*, 154.
33. Bhatia, V.; Barber, R. *J. Am. Pharm. Assoc.* **1955**, *44*, 342.
34. Pal, K.; Banthia, A. K.; Majumdar, D. K. *AAPS PharmSciTech* **2007**, *8*, 142.
35. Pal, K.; Banthia, A.; Majumdar, D. *J. Mater. Sci. Mater. Med.* **2007**, *18*, 1889.
36. Pal, K.; Pal, S. *Mater. Manuf. Process.* **2006**, *21*, 325.
37. Pal, K.; Banthia, A.; Majumdar, D. *Biomed. Mater.* **2006**, *1*, 85.
38. Sutar, P. B.; Mishra, R. K.; Pal, K.; Banthia, A. K. *J. Mater. Sci. Mater. Med.* **2008**, *19*, 2247.
39. Pal, K.; Bag, S.; Pal, S. *J. Porous Mater.* **2008**, *15*, 53.
40. Pal, K.; Bag, S.; Pal, S. *Trends Biomater. Artif. Organs* **2005**, *19*, 39.
41. Roy, S.; Pal, K.; Thakur, G.; Prabhakar, B. *Mater. Manuf. Process.* **2010**, *25*, 1477.
42. Behera, B.; Patil, V.; Sagiri, S.; Pal, K.; Ray, S. *J. Appl. Polym. Sci.* **2012**, *125*, 852.
43. Sagiri, S. S.; Behera, B.; Sudheep, T.; Pal, K. *Des. Monomers Polym.* **2012**, *15*, 253.
44. Shibayama, M.; Hiroyuki, Y.; Hidenobu, K.; Hiroshi, F.; Shunji, N. *Polymer* **1988**, *29*, 2066.
45. Gupta, S.; Pramanik, A. K.; Kailath, A.; Mishra, T.; Guha, A.; Nayar, S.; Sinha, A. *Colloids Surf. B* **2009**, *74*, 186.
46. Tzeng, B. C.; Schier, A.; Schmidbaur, H. *Inorg. Chem.* **1999**, *38*, 3978.
47. Focher, B.; Naggi, A.; Torri, G.; Cosani, A.; Terbojevich, M. *Carbohydr. Polym.* **1992**, *18*, 43.
48. Shirakawa, M.; Kawano, S.; Fujita, N.; Sada, K.; Shinkai, S. *J. Org. Chem.* **2003**, *68*, 5037.
49. Bhattacharya, S.; Pal, A. *J. Phys. Chem. B* **2008**, *112*, 4918.
50. Terech, P.; Allegraud, J.; Garner, C. *Langmuir* **1998**, *14*, 3991.
51. Dassanayake, L. S. K.; Kodali, D. R.; Ueno, S.; Sato, K. *J. Am. Oil Chem. Soc.* **2009**, *86*, 1163.
52. Sawalha, H.; Venema, P.; Bot, A.; Flöter, E.; van der Linden, E. *Food Biophys.* **2011**, *6*, 20.
53. Abdallah, D. J.; Lu, L.; Weiss, R. G. *Chem. Mater.* **1999**, *11*, 2907.
54. Abdallah, D. J.; Weiss, R. G. *Chem. Mater.* **2000**, *12*, 406.
55. Da Pieve, S.; Calligaris, S.; Panozzo, A.; Arrighetti, G.; Nicoli, M. C. *Food Res. Int.* **2011**, *44*, 2978.
56. Rooki, R.; Ardejani, F. D.; Moradzadeh, A.; Kelessidis, V. C.; Nourozi, M. *Int. J. Mineral Process.*
57. Møller, P.; Fall, A.; Bonn, D. *Europhys. Lett.* **2009**, *87*, 38004.

58. Sousa, P.; Coelho, P.; Oliveira, M.; Alves, M. *Chem. Eng. Sci.* **2011**, *66*, 998.

59. Afanasiev, K.; Münch, A.; Wagner, B. *Phys. Rev. E* **2007**, *76*, 036307.

60. Kamble, S.; Udapurkar, P.; Biyani, K.; Nakhat, P.; Yeole, P. Inventi Rapid: NDDS; Inventi Journals (P) Ltd: Bhopal, India, **2011**.

61. Jadhav, K. R.; Kadam, V. J.; Pisal, S. S. *Curr. Drug Delivery* **2009**, *6*, 174.

62. Zhang, J.; Wu, M.; Qin, Y.; Chen, R.; Jiang, Y.; Sun, Y.; Yang, Z. *Acta Physicochim. Sinica* **2008**, *24*, 79.

63. Fukushima, T.; Aida, T. *Chem. A Eur. J.* **2007**, *13*, 5048.

64. Raval, A.; Parikh, J.; Engineer, C. *Ind. Eng. Chem. Res.* **2011**, *50*, 9539.

65. Schmid-Wendtner, M. H. PH and Skin Care; Abw Wissenschaftsverlag: Berlin, Germany, **2007**.

66. Bhatia, V. N.; Barber, R. H. *J.Am. Pharm. Assoc.* **1955**, *44*, 342.

67. Paulusse, J. M. J.; van Beek, D. J. M.; Sijbesma, R. P. *J. Am. Chem. Soc.* **2007**, *129*, 2392.

68. Yosipovitch G, H. *J. HMP Commun.* **2003**, *11*, 88.

69. Dutta, P.; Dey, J.; Perumal, V.; Mandal, M. *Int. J. Pharm.* **2011**, *407*, 207.

70. Raut, S.; Bhadoriya, S. S.; Uplanchiwar, V.; Mishra, V.; Gahane, A.; Jain, S. K. *Acta Pharm. Sinica B* **2012**, *2*, 8.